nature geoscience

BRIEF COMMUNICATION

https://doi.org/10.1038/s41561-021-00869-z

Tsunami size variability with rupture depth

Kwok Fai Cheung[1]✉, Thorne Lay[2], Lin Sun[1,3] and Yoshiki Yamazaki[1]

Observed maximum water heights from tsunamis vary by up to two orders of magnitude for a given earthquake size, presenting a challenge to emergency management. We provide a quantitative framework to investigate the influence of rupture depth and rigidity in explaining such variability. The results highlight the importance of rapid estimation of shallow slip with available geophysical data if reliable warning of local tsunamis is to be realized.

Researchers have long questioned the use of earthquake magnitude alone to gauge tsunami size and have proposed additional independent rapid measures for local tsunami warning[1]. The issue is illustrated by plotting observed maximum water heights against seismic moment magnitude, M_w, for recent interplate thrust earthquakes[2]. The mix of tide-gauge and run-up observations in Fig. 1 exhibits up to two orders of magnitude variability for a given M_w and shows a clear tendency for shallow-rupturing earthquakes to produce larger tsunamis. Local amplification of extreme run-up and limited tide-gauge coverage of small events contribute to the variability, but the tectonic processes represent the key factor. A special class of events known as tsunami earthquakes[3], which produce very large tsunamis for their M_w, exemplifies this behaviour. Seismic imaging supports the presence of substantially reduced rigidity around the shallow megathrust[4]. Shallow rupture with low rigidity produces relatively weak ground shaking, and at a given seismic moment leads to enhanced seafloor deformation for tsunami excitation[5,6].

A simplified megathrust model is used to investigate the role of M_w as well as the influences of rupture depth and rigidity in determining tsunami size (Methods). The inset in Fig. 1 shows the model cross section consisting of an abyssal plain, an upper plate seafloor slope and an along-trench fault for pure thrust earthquakes. The model with a straight shoreline is not intended to match observed maximum run-up heights, which may be locally amplified by factors of up to 2.5 from the overall run-up heights estimated within source regions. We initially consider a single-segment fault with width and length determined from scaling relations[7] in terms of M_w. The non-hydrostatic model NEOWAVE[8] describes tsunami generation and propagation from the resulting seafloor deformation. Figure 1 shows the computed maximum sea surface elevation for 40 GPa rigidity typical of the deeper part of the megathrust[9]. A reference depth (up-dip slip limit) of 20 km can account for most tide-gauge-recorded tsunamis of less than ~1 m amplitude generated by earthquakes with $M_w \leq 8.2$ that have no shallow slip. The computed sea surface elevation appears to saturate between 0 and 15 km reference depth, exhibiting minor overlap with the overall run-up heights. As the magnitude increases, the wider fault extends below dry land, truncating the energy contributing to the tsunami. Such effects become most prominent for zero reference depth and small dip angles due to occurrence of large subsidence on dry land as well as moderate and uniform uplift over most of the remaining fault.

Recent finite-fault studies of some seismic events have revealed that concentrated large near-trench slip is responsible for the resulting tsunami impact[10,11]. Halving the fault width and doubling the slip to hold M_w fixed reduces the portion of the fault under dry land for large events and shifts the seafloor deformation to deeper water in all cases. Apart from larger tsunami excitation, the resulting waves with shorter period in deeper water undergo a longer shoaling process that gains more amplitude before reaching the shore. For 0–15 km reference depth and 40 GPa rigidity, Fig. 2 shows a distinct band of computed maximum sea surface elevation above the baseline established for deeper earthquakes. Shallow ruptures from the trench to 15 km below the sea surface can involve rigidity as low as 5 GPa (ref. [9]). A two-segment fault can accommodate such reduced rigidity in shallow rupture, while retaining 40 GPa in the deeper segment if present. The correspondingly increased slip in the shallow portion of the fault for the fixed moment calculations accounts for sea surface elevations with up to two orders of magnitude variability. There is overlap of the results obtained from ranges of reference depth, fault dip and rigidity for $M_w < \sim 7.8$ because the tsunami excitation attenuates over the water column, depending on the deformed seafloor area. As the fault dimensions increase with earthquake magnitude, these non-hydrostatic effects become less pronounced in the generation process. There is a clear tendency for shallow rupture with low rigidity to produce large tsunamis for a given M_w.

The maximum run-up heights in Fig. 2 are influenced by local topography not accounted for by the simplified megathrust model. Additional analysis and interpretation are needed when comparing the observed and computed data, especially for extreme events. The observed maximum run-up height of ~40 m from the 2011 Tohoku tsunami, which is outside the range of plausible models, is a result of local amplification at the rugged Sanriku coast. The estimated overall run-up height in the source region suggests 20 GPa rigidity for the shallow portion of the M_w 9.1 earthquake rupture. The present model gives ~20–30 m of maximum sea surface elevation generated by 37 and 18.5 m of slip in the shallow and deep fault segments, corroborating the results from high-resolution modelling of the tsunami[11]. Similarly, the observed run-up from the 2010 Mentawai tsunami reaches 10 m along most of the severely impacted shorelines but a maximum of 16.9 m at a topographic feature[12]. The 10 m overall run-up height is in the band of maximum sea surface elevation computed for 10 GPa rigidity in the shallow megathrust, and the corresponding slip of 17 m in a narrow fault segment for the M_w 7.9 tsunami earthquake gives good agreement with joint inversion of tsunami and seismic data[10]. The 1998 Papua New Guinea earthquake is a notable outlier that triggered large tsunamigenic submarine slumps. The resulting tsunami is well outside the model coverage even with the lower-bound rigidity of 5 GPa.

DART (Deep-ocean Assessment and Reporting of Tsunamis) data have been instrumental for warning of trans-oceanic tsunamis

[1]Department of Ocean and Resources Engineering, University of Hawaii at Manoa, Honolulu, HI, USA. [2]Department of Earth and Planetary Sciences, University of California, Santa Cruz, CA, USA. [3]Presently at ControlPoint Surveying, Inc., Honolulu, HI, USA. ✉e-mail: cheung@hawaii.edu

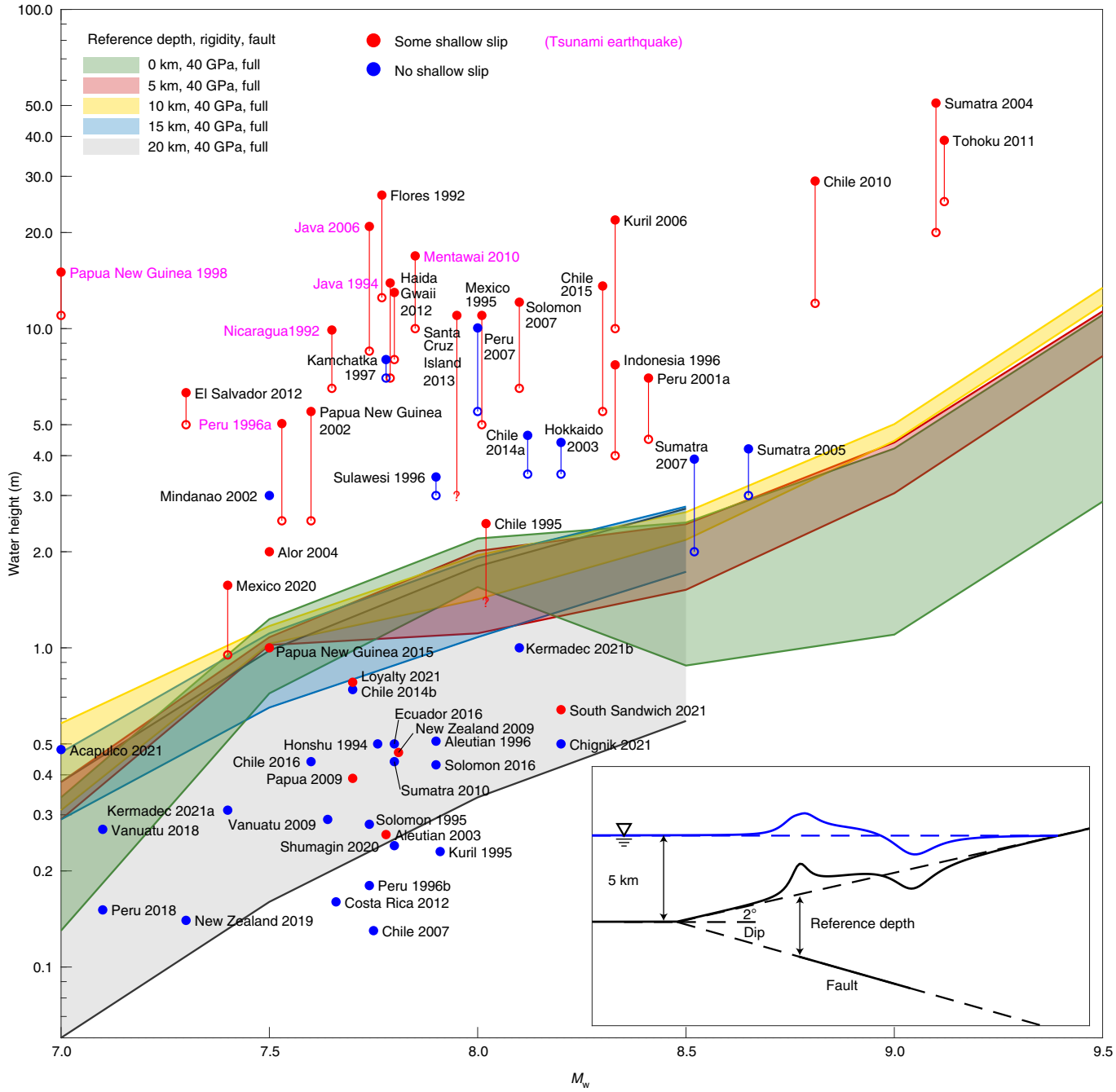

Fig. 1 | Observed water heights and computed maximum sea surface elevations with 40 GPa rigidity versus M_w. Solid circles denote observed maximum water heights colour coded by independent source investigations of whether some shallow slip occurred[2], with tsunami earthquakes[3] highlighted in magenta. Open circles indicate estimates of overall observed run-up heights within source regions. Each colour band spans the computations for plausible models with 5° to 25° dip angles and full fault width.

but are of limited use for communities near the source. Our systematic quantification of tsunami size dependence on M_w and rupture depth, accounting for rigidity and slip trade-off, emphasizes a major challenge confronting rapid near-source tsunami warning efforts. While rapid determination of M_w by analysis of nearby long-period seismic motions is now viable[13], and land-based high-rate geodetic observations can constrain along-strike extent and deep fault slip close to shore[1], these approaches do not resolve whether large shallow slip on the megathrust occurred far offshore. Presence or absence of such slip can produce up to two orders of magnitude variability in maximum water height for a given M_w. Finite-fault seismic inversions can resolve shallow slip correctly only if appropriate low rigidity is incorporated in the waveform modelling, which requires prior availability of high-resolution near-trench seismic velocity structures[4]. New seismological and seafloor geodesy approaches that can rapidly determine the up-dip limit and amount of coseismic slip on the megathrust[2] are of great importance to improving the accuracy of tsunamigenic assessment as well as to determining the along-dip variation in source-region properties for plate boundary megathrusts.

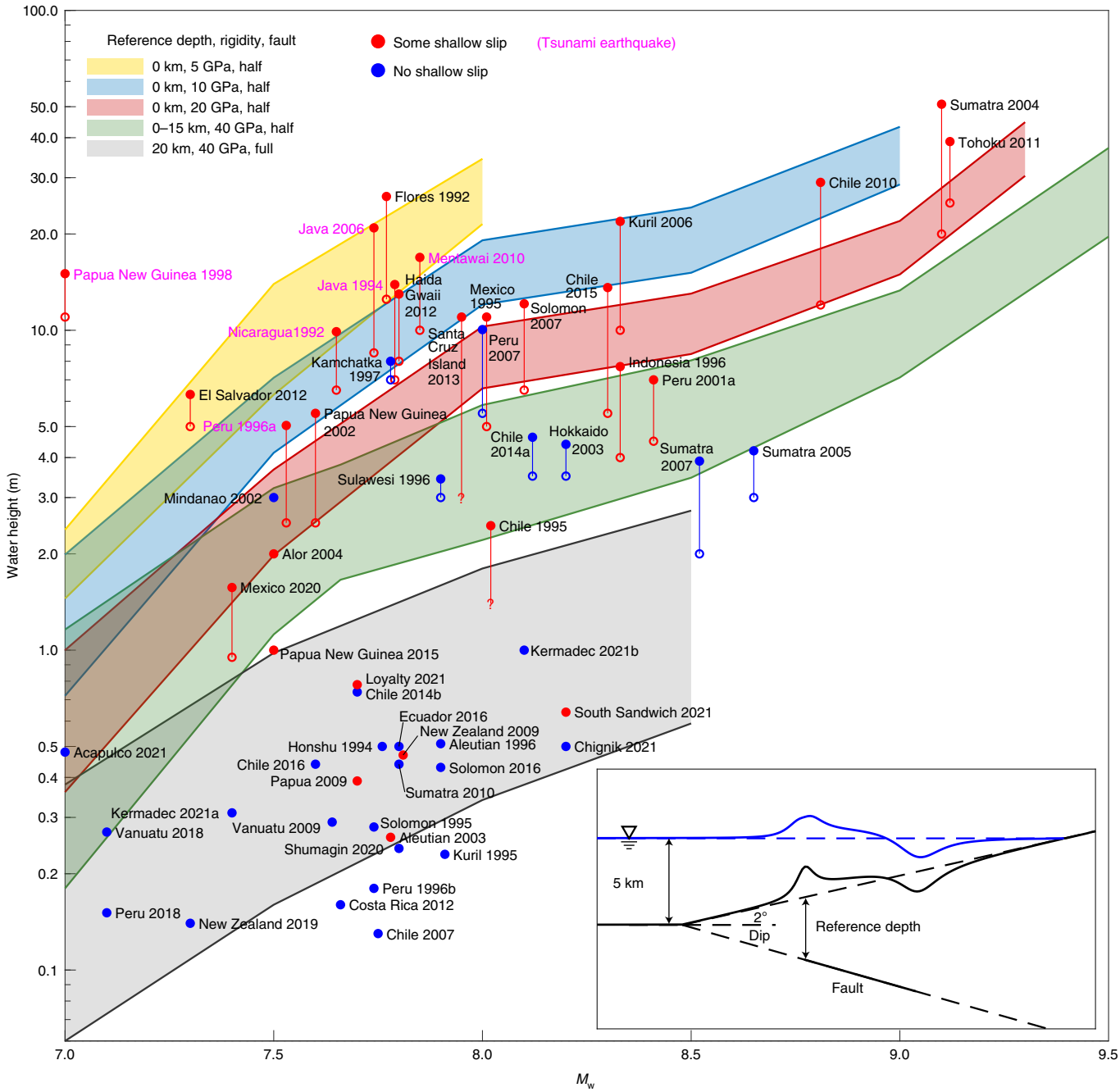

Fig. 2 | Observed water heights and computed maximum sea surface elevation with variable rigidity versus M_w. Reduced rigidity of 5, 10 and 20 GPa is used for the shallow portion of ruptures from the trench to 15 km below sea surface instead of 40 GPa. Solid circles denote observed maximum water heights colour coded by independent source investigations of whether some shallow slip occurred[2], with tsunami earthquakes[3] highlighted in magenta. Open circles indicate estimates of overall observed run-up heights within source regions. Each colour band spans the computations for plausible models with 5° to 25° dip angles and full or half fault width.

Online content

Any methods, additional references, Nature Research reporting summaries, source data, extended data, supplementary information, acknowledgements, peer review information; details of author contributions and competing interests; and statements of data and code availability are available at https://doi.org/10.1038/s41561-021-00869-z.

Received: 15 June 2020; Accepted: 9 November 2021;
Published online: 13 December 2021

References

1. Melgar, D. et al. Local tsunami warnings: perspectives from recent large events. *Geophys. Res. Lett.* **43**, 1109–1117 (2016).
2. Lay, T., Liu, C. & Kanamori, H. Enhancing tsunami warning using *P* wave coda. *J. Geophys. Res. Solid Earth* **124**, 10583–10609 (2019).
3. Kanamori, H. Mechanism of tsunami earthquakes. *Phys. Earth. Planet. Inter.* **6**, 346–359 (1972).
4. Sallarés, V. & Ranero, C. R. Upper-plate rigidity determines depth-varying rupture behaviour of megathrust earthquakes. *Nature* **576**, 96–101 (2019).
5. Polet, J. & Kanamori, H. Shallow subduction zone earthquakes and their tsunamigenic potential. *Geophys. J. Int.* **142**, 684–702 (2000).

6. Bilek, S. & Lay, T. Tsunami earthquakes possibly widespread manifestations of frictional conditional stability. *Geophys. Res. Lett.* **29**, 1673 (2002).
7. Allen, T. I. & Hayes, G. P. Alternative rupture-scaling relationships for subduction interface and other offshore environments. *Bull. Seismol. Soc. Am.* **107**, 1240–1253 (2017).
8. Yamazaki, Y., Kowalik, Z. & Cheung, K. F. Depth-integrated, non-hydrostatic model for wave breaking and run-up. *Int. J. Numer. Methods Fluids* **61**, 473–497 (2009).
9. Lay, T. et al. Depth-varying rupture properties of subduction zone megathrust faults. *J. Geophys. Res. Solid Earth* **117**, B04311 (2012).
10. Li, L. et al. Effects of dispersion in tsunami Green's functions and implications for joint inversion with seismic and geodetic data: a case study of the 2010 Mentawai M_w 7.8 earthquake. *Geophys. Res. Lett.* **43**, 182–11,191 (2016).
11. Yamazaki, Y., Cheung, K. & Lay, T. A self-consistent fault slip model for the 2011 Tohoku earthquake and tsunami. *J. Geophys. Res. Solid Earth* **123**, 1435–1458 (2018).
12. Hill, E. M. et al. The 2010 M_w 7.8 Mentawai earthquake: very shallow source of a rare tsunami earthquake determined from tsunami field survey and near-field GPS data. *J. Geophys. Res. Solid Earth* **117**, B006402 (2012).
13. Kanamori, H. & Rivera, L. Source inversion of W phase: speeding up seismic tsunami warning. *Geophys. J. Int.* **175**, 222–238 (2008).

Methods

The simplified megathrust model comprises an abyssal plain with a uniform water depth of 5 km, an upper plate seafloor slope of 2° and a plate interface with a constant dip angle as shown in Figs. 1 and 2. The rectangular fault has an along-trench strike with 90° rake, and its length and width in kilometres are determined from scaling relations[7]

$$\log L = -2.9 + 0.63M_w \quad (1)$$

$$\log W = \begin{cases} -1.91 + 0.48M_w & \text{for } M_w \leq 8.67 \\ 2.29 & \text{for } M_w > 8.67 \end{cases} \quad (2)$$

in which

$$M_w = \frac{2}{3}\log M_0 - 6.03 \quad (3)$$

where the seismic moment M_0 is the product of rigidity, rupture area and average slip[14,15]. An elastic half-space solution[16] determines the seafloor deformation from the fault dimensions, slip, reference depth and an effective dip angle including the seafloor slope. The vertical seafloor displacement is corrected for the horizontal motion of the slope for tsunami modelling[17].

NEOWAVE[8] is a depth-integrated non-hydrostatic model utilizing a vertical velocity term to attain wave dispersion comparable to low-order Boussinesq-type equations[18,19]. The vertical velocity term also facilitates modelling of tsunami generation from seafloor displacement over a finite rise time[20], which is assumed to be 15 s in this study. The process accounts for attenuation of the seafloor excitation over the water column to provide a more realistic description of near-field tsunamis. The rectangular computational domain is 1,000 km wide centred at the trench and 800–1,600 km long depending on M_w, with a Manning roughness coefficient of 0.025. A sensitive analysis shows a cell size of 0.5 km by 0.5 km is sufficient to resolve wave shoaling on the slope and reflection from the featureless shoreline for the parametric study.

The parameter space covers 5–25° dip angle, 0–20 km reference depth, 5–40 GPa rigidity, M_w 7.0–9.5 and fault widths of W and $W/2$. The computed maximum sea surface elevations from the dip-angle range are grouped for presentation. The lower and upper bounds are typically defined by 5° and 25°, but the trend reverses for low-magnitude earthquakes due to dominance of non-hydrostatic effects. When rigidity ≤20 GPa is considered for shallow rupture[9], fault slip below 15 km from sea surface is computed using 40 GPa, assuming uniform moment distribution. The increased shallow slip leads to an upper bound defined by ~10–15° dip angle. The models are truncated at M_w 8.5 for reference depth ≥15 km with full fault width due to reduced probability and when the shallow slip reaches ~60 m, corresponding to the observed upper limit for the M_w 9.1 Tohoku earthquake[21,22].

Observed water heights from tsunamis generated by large interplate thrust earthquakes between 1990 and 2021 are compiled from the Global Historic Tsunami Database[23]. The dataset is updated from a previous study[2] through 2021 with additional sorting for the maximum water heights by excluding splash and far-field observations. The run-up observations at each source region are analysed and cross referenced with available publications to estimate an overall run-up height, which is equivalent to an average after excluding localized high and low values, for more ready comparison with the computed maximum sea surface elevation.

Data availability

The processed water heights from observations and model data in Figs. 1 and 2 are available at https://doi.org/10.6084/m9.figshare.16944163.

Code availability

The megathrust model and code, specifically set up for this study, are available for academic research upon request.

References

14. Aki, K. Generation and propagation of G waves from the Niigata earthquake of June 16, 1964: part 2. estimation of earthquake moment, released energy, and stress-strain drop from the G wave spectrum. *Bull. Earthq. Res. Inst.* **44**, 73–88 (1966).
15. Kanamori, H. The energy release in great earthquakes. *J. Geophys. Res.* **82**, 2981–2987 (1977).
16. Okada, Y. Surface deformation due to shear and tensile faults in a half-space. *Bull. Seismol. Soc. Am.* **75**, 1125–1154 (1985).
17. Tanioka, Y. & Satake, K. Tsunami generation by horizontal displacement of ocean bottom. *Geophys. Res. Lett.* **23**, 861–864 (1996).
18. Bai, Y., Yamazaki, Y. & Cheung, K. F. Convergence of multilayer nonhydrostatic models in relation to Boussinesq-type equations. *J. Waterw. Port Coast. Ocean Eng.* **14**, 06018001–06018001 (2018).
19. Li, L. & Cheung, K. F. Numerical dispersion in non-hydrostatic modeling of long-wave propagation. *Ocean Model.* **138**, 68–87 (2019).
20. Yamazaki, Y., Cheung, K. F. & Kowalik, Z. Depth-integrated, non-hydrostatic model with grid nesting for tsunami generation, propagation, and run-up. *Int. J. Numer. Methods Fluids* **67**, 2081–2107 (2011).
21. Fujiwara, T. et al. The 2011 Tohoku-Oki earthquake: displacement reaching the trench axis. *Science* **334**, 1240 (2011).
22. Ito, T., Ozawa, K., Watanabe, T. & Sagiya, T. Slip distribution of the 2011 off the Pacific coast of Tohoku earthquake inferred from geodetic data. *Earth Planets Space* **63**, 627–630 (2011).
23. Global Historical Tsunami Database, *US National Centers for Environmental Information, World Data Service*, https://doi.org/10.7289/V5PN93H7 (2021).

Acknowledgements

We acknowledge support from the US National Oceanic and Atmospheric Administration through NA19NWS4670012 (K.C., Y.Y. and L.S.) and National Science Foundation through EAR1802364 (T.L.). SOEST contribution no. 11418.

Author contributions

K.C. and T.L. conceived the study and wrote the draft manuscript; Y.Y. customized NEOWAVE for implementation; L.S. carried out the tsunami modelling and data processing; and all authors worked collaborative to interpret the data and finalize the manuscript for publication.

Competing interests

The authors declare no competing interests.

Additional information

Correspondence and requests for materials should be addressed to Kwok Fai Cheung.

Peer review information *Nature Geoscience* thanks Kelin Wang and Aditya Gusman for their contribution to the peer review of this work. Primary Handling Editors: Stefan Lachowycz; Rebecca Neely.

Reprints and permissions information is available at www.nature.com/reprints.